European Review for Medical and Pharmacological Sciences 2021; 25: 313-325

Differential response of cardiac aquaporins to hyperosmotic stress; salutary role of AQP1 against the induced apoptosis

I.-K. AGGELI, A. KAPOGIANNATOU, F. PARASKEVOPOULOU, C. GAITANAKI

[1]Section of Animal and Human Physiology, Faculty of Biology, School of Science, National and Kapodistrian University of Athens, University Campus, Ilissia, Athens, Greece

Aspasia Kapogiannatou and Foteini Paraskevopoulou contributed equally

Abstract. – OBJECTIVE: Multiple pathophysiological conditions are associated with disturbance of myocardial osmotic equilibrium, exerting detrimental effects on cardiac performance. Cardiac myocytes may encounter hyperosmotic stress during hyperglycemia, ischemia/reperfusion injury, myocardial infarction, diabetes mellitus, severe dehydration, hypoxia or heat stress. Aquaporins (AQPs) constitute transmembrane channels that facilitate water transport in response to osmotic gradients. Therefore, the present study aimed at probing into AQPs mode of response and potential role as effector molecules and sensors, under hyperosmotic stress.

MATERIALS AND METHODS: H9c2 cardiac myoblasts were left untreated (control) or were exposed to 0.5 M sorbitol so as to induce hyperosmotic stress conditions. After the experimental treatments, MTT assay was performed to assess cell viability. Endogenous mRNA levels of AQP1 and AQP7 were assessed by ratiometric RT-PCR. Their subcellular localization pattern was revealed by immunofluorescence microscopy. Protein levels of AQP1 and AQP7, as well as of apoptotic markers (cleaved caspase-3 and PARP), were detected by immunoblot analysis.

RESULTS: Hyperosmotic stress (0.5 M sorbitol) induced a time-dependent upregulation of AQP7 (but not of AQP1) mRNA in H9c2 cells. Of note, biochemical and immunocytochemical analyses revealed the increased membrane-associated protein expression of AQP1, under these conditions, while AQP7 respective levels remained unchanged. Interestingly, inhibition of AQP1 by $HgCl_2$, aggravated the sorbitol-induced apoptosis in H9c2 cells, as evidenced by chromatin condensation and fragmentation of caspase-3 and PARP.

CONCLUSIONS: AQP1 and AQP7 are differentially regulated under hyperosmotic stress conditions in H9c2 cells. AQP1, acting as an osmotic stress sensor and response factor, exerts a beneficial effect against the sorbitol-induced apoptosis, potentially favoring preservation of cardiac function.

Key Words:
Aquaporin, Hyperosmotic stress, H9c2 cardiac myoblasts, Apoptosis.

Abbreviations

AQP, aquaporin; BSA, bovine serum albumin; DMSO, dimethyl sulphoxide; DTT, ditheiothreitol; ECL, enhanced chemiluminescence; MAPK, mitogen-activated protein kinase; PARP, poly(ADP-ribose) polymerase; ROS, reactive oxygen species; TBS, Tris-buffered saline.

Introduction

Cardiovascular diseases constitute the principal cause of death in developed countries. Osmotic perturbations may result in impairment of cardiac performance. This is evidenced in several conditions of clinical importance, i.e., hyperglycemia, hyperlipidemia, diabetes mellitus, severe dehydration, hypoxia, heat stress, ischemia/reperfusion injury, myocardial infarction, hypoxia, cardioplegia or cardiopulmonary bypass surgery[1]. Even minor imbalances of the osmotic equilibrium may lead to development of myocardial edema, with detrimental effects on heart microcirculation and metabolism. The induced myocardial stunning and cell death exacerbate cardiac function[2,3]. Evidently, revealing the salutary role of any effector molecules that function as osmotic stress sensors and response factors is of fundamental significance.

Water is transported through lipid bilayers by simple diffusion or via selective water pores. In 2003, Peter Agre was awarded the Nobel Prize in Chemistry, for the discovery of aquaporins (AQPs), the transmembrane channels that facilitate water

Corresponding Author: Ioanna-Katerina Aggeli, Ph.D; e-mail: ikaggeli@biol.uoa.gr

transport in response to osmotic gradients[4]. Thirteen isoforms have been identified so far in mammals, with AQP1, -2, -4, -5, -6, -8, -12 and -0 being selective for water and AQP3, -7, -9, -10 and -11 also allowing passage of glycerol. Certain isoforms also facilitate transport of ammonia, urea, carbon dioxide and hydrogen peroxide, thereby contributing to waste metabolism, gas exchange and trafficking of signaling effectors[5]. AQPs exist as tetramers with each monomer having its own pore and a molecular mass of ~28 kDa. Although AQPs are ubiquitously expressed in many renal and non-renal tissues, those of kidney and brain have monopolized the interest of researchers.

Consequently, the role of cardiac AQPs remains elusive, since reports on their cellular distribution and expression vary significantly, depending on species examined and the techniques applied. With respect to rat cardiac tissue, transcripts of several AQPs have been detected (AQP1, -3, -4, -5, -6, -7, -11), but only a few at protein level, with AQP1 expression being the most prominent[1]. So far, most reports on cardiac AQPs have focused on AQP1 and several on AQP7. In particular, AQP1 has been found to mediate transepithelial water flux and hydrogen peroxide exchange[5]. Calcium influx, calmodulin and PKC-dependent phosphorylation have been shown to regulate subcellular localization of AQP1[6]. As far as AQP7 is concerned, its deficiency appears to compromise metabolic adaptation upon cardiac overload, via limitation of glycerol uptake and reduction of intracellular ATP levels[7]. This is of fundamental significance, since metabolism of cardiac myocytes relies on fatty acids, but shifts to glucose and glycerol as energy substrates, under cardiac overload.

Diverse regulatory mechanisms orchestrate the activity, function and localization of AQPs. In particular, abundance and properties of AQPs can be regulated: a) at gene and/or protein levels, b) by receptor-mediated mechanisms[8] and c) by modifications in their membrane expression levels[6]. There is also evidence that the potential role of AQPs in preservation of myocardial water balance may determine the clinical outcome of several cardiovascular diseases. Therefore, gaining insight into the molecular mechanisms that regulate their responses is critical.

Overall, the present study unveils the differential mode of regulation of AQP1 and AQP7 in H9c2 cardiac myoblasts exposed to hyperosmotic stress, with emphasis on the beneficial role of AQP1 against the apoptotic mechanism triggered. Our findings highlight AQP1 as a promising effector molecule that may attenuate myocardial deterioration and progression of cardiovascular pathologies. H9c2 cells constitute an established experimental model, widely used to investigate the signalling mechanisms and pathways involved in ischemia, ischemia/reperfusion, hypoxia, autophagy, hypertrophy, apoptosis, endoplasmic reticulum-mitochondria interactions and cellular stress responses in cardiac myocytes. In addition, the energy metabolism profile identified in H9c2 cells makes them an excellent experimental alternative in studies simulating cellular stress conditions, including osmotic imbalances.

Materials and Methods

Reagent and Antibodies

Dithiothreitol (DTT), phenylmethylsulphonyl fluoride (PMSF), dimethyl sulfoxide (DMSO), sorbitol, thiazolyl blue tetrazolium bromide (MTT) and Bradford protein assay reagent were purchased from AppliChem GmbH (Darmstadt, Germany). Leupeptin, trans-epoxy succinyl-L-leucyl amido-(4-guanidino) butane (E-64), Nonidet P-40 were from Merck (Burlington, MA, USA). $HgCl_2$ was purchased from Acros Organics (part of Thermo Fisher Scientific, Geel, Belgium).

Nitrocellulose (0.45 μm) was obtained from Macherey-Nagel GmbH (Duren, Germany). Prestained molecular mass markers were from New England Biolabs (Beverly, MA, USA). The rabbit polyclonal antibodies for poly (ADP-ribose) polymerase (PARP) (#9542) and caspase-3 (#9662) were purchased from Cell Signaling Technology (Beverly, MA, USA), while rabbit polyclonal anti-actin (A2103), as well as anti-Gs alpha (G5040) antibodies, were from Merck. Rabbit polyclonal anti-AQP1 antibody (RA3391/2353) and anti-AQP7 antibody (RA2900/1246) were a kind gift from Prof. S. Nielsen (University of Aarhus, Aarhus, Denmark). The peroxidase-conjugated goat anti-rabbit IgG secondary antibody was from Merck (Burlington, MA, USA) and the goat anti-rabbit IgG-FITC secondary antibody from Santa Cruz Biotechnology (Dallas, TX, USA). The enhanced chemiluminescence (ECL) kit was from GE Healthcare (Buckinghamshire, UK). Super RX film was purchased from Fuji photo film GmbH (Dusseldorf, Germany). Cell culture supplies were from PAA Laboratories (Pasching, Austria). Hoechst 33258 was from Invitrogen (part of Thermo Fisher Scientific, Waltham, MA, USA).

Cell Culture and Treatments

H9c2 rat cardiac myoblasts (passage 18-25; American Type Culture Collection CRL-1446, Manassas, VA, USA) were grown in high glucose (4.5g/L) Dulbecco's Modified Eagle's Medium (DMEM; Gibco, Paisley, UK), in the presence of 10% (v/v) fetal bovine serum (FBS; Thermo-Fischer Scientific, Waltham, MA, USA) and penicillin-streptomycin (1:100; Thermo Fischer Scientific, Waltham, MA, USA), under a humidified atmosphere of 95% air/5% CO_2 at 37°C, with mycoplasma testing routinely performed. Cells were seeded in 60-mm dishes and grown to approximately 70% confluence. Before any treatment, serum had been withdrawn for at least 18 h. Sorbitol (0.5 M) was added to the medium for the times indicated.

Cell Viability Assay

The number of viable cells was determined using the 3-(4,5-dimethylthiazol-2-yl)-2,5-diphenyltetrazolium bromide (MTT) assay. After seeding cells in 96-well culture plates ($5x10^3$cells/well), they were treated with various concentrations of $HgCl_2$ for 24 h. Untreated cells were used as controls. Four hours before the end of treatment, 50 μg MTT was added to each well. Next, the medium was aspirated, cells were lysed in 0.1 M HCl/isopropanol to dissolve the reduced MTT formazan crystals and absorbance was measured in an ELISA microplate reader (DENLEY, West Sussex, UK) using a 545-nm filter. All experiments were performed in triplicate.

RNA Preparation, cDNA Synthesis and Ratiometric Reverse Transcription PCR (RT-PCR)

Ratiometric reverse transcription of total RNA followed by PCR analysis were performed to analyze the expression of endogenous AQPs. Total RNA was extracted from H9c2 cells using TRIzol (Invitrogen, Carlsbad, CA, USA), followed by cDNA synthesis in which 2 μg of total RNA was denatured in the presence of 5 pmoles oligo-dT primer in a reaction volume of 13.5 μl (65°C, 5 min). PCR for AQP1 was performed using 1.5 Units Taq (Bioron GmbH, Ludwigshafen, Germany) with sense 5'-CTTACCTCCAGGACCCTTCC-3' and antisense 5'-TAGCTCATCCACACGTGCTC-3' primers, based on the sequence of rat AQP1 [GenBank Accession No. NM_012778]. These primers amplify a 232-base pair PCR product. AQP7 primers were as follows: sense 5'-ATCCTTGTTTGCGTTCTTGG-3' and antisense 5'-GCGTGAATTAAGCCCAGGTA-3' based on the sequence of rat AQP7, for a 212-base pair PCR product [GenBank Accession No. NM_ 019157]. PCR was carried out for 27 cycles (94°C for 30 sec, 59°C for 30 sec and 72°C for 30 sec) with the final extension performed at 72°C (4 min). PCR (25 cycles) for GAPDH was performed using the following primers: sense 5'-ACC ACA GTC CAT GCC ATC AC-3' and antisense 5'-TCC ACC ACC CTG TTG CTG TA-3' [GenBank Accession No. X02231]. cDNA samples derived from untreated (control) and treated cells were always amplified simultaneously. PCR products were separated on a 2% (w/v) agarose gel and band intensities were determined using Gel Analyzer v. 1.0. All values were normalized for the amount of GAPDH mRNA. Negative controls included samples where template was omitted.

Preparation of Protein Extracts

Following treatment, the cells were washed twice in ice-cold phosphate-buffered saline (PBS) and harvested by scraping the dishes. To prepare soluble (cytoplasmic) and particulate (membrane) fractions, H9c2 cells were scraped into ice-cold buffer (12.5 mM Tris-HCl, pH 7.4, 2.5 mM EGTA, 1 mM EDTA, 50 mM NaF, 5 mM dithiothreitol, and 0.5 mM PMSF, with 2 μg/ml leupeptin, 2 μM microcystin, and 10 μM E64). Samples were centrifuged in a BR4i Jouan centrifuge (10.000 g, 10 min, 4°C) and the soluble fractions were collected. The pellets were resuspended in 100 μl of the aforementioned buffer containing 2% (v/v) Triton X-100. They were next incubated on ice for 15 min and the solubilized particulate fractions were collected following centrifugation (20.800 g, 10 min, 4°C). Protein concentration was determined using the Bradford assay. After quantification, 0.33 vol. of Sample Buffer [SB4X: 0.33 mol/l Tris-HCl (pH 6.8), 10% (w/v) SDS, 13% (v/v) glycerol, 20% (v/v) 2-mercaptoethanol, 0.2% (w/v) bromophenol blue] was added to the samples, which were then boiled and stored at -20°C until use. For the evaluation of caspase-3 activation, Chaps buffer [50 mM HEPES/KOH pH 6.5, 2 mM EDTA, 0.1% (w/v) Chaps, 20 μg/ml leupeptin, 5 mM DDT, 1 mM PMSF, 10 μg/ml aprotinin and 10 μg/ml pepstatin A] was used. Next, the samples were repeatedly frozen [−80 °C (×3)] and left to thaw. Lysates were then centrifuged (20.800 g, 4°C, 20 min) and protein concentrations were determined using the Bradford assay. Samples were then boiled with 0.33 vol. of SB4X. For whole cell extracts, H9c2 cells were

lysed in ice-cold buffer [20 mM Tris-HCl pH 7.5, 20 mM β-glycerophosphate, 2 mM EDTA, 10 mM benzamidine, 20 mM NaF, 0.2 mM Na_3VO_4, 200 μM leupeptin, 10 μM E-64, 5 mM DTT, 300 μM PMSF and 0.5% (v/v) Triton X-100], and then, incubated on ice for 15 min. Lysates were centrifuged (20.800 g, 10 min, 4°C) and the supernatant (total protein extract) was collected. Protein concentration was determined using the Bradford assay. After quantification, 0.33 vol. of SB4X was added to the samples, which were then boiled and stored at -20°C until use.

Chromatin Condensation Assay

H9c2 cells were cultured onto ibidi (Martinsried, Germany) 4-well μ-slides and treated with 0.5 M sorbitol for 1 h in the presence or absence of $HgCl_2$ (25μM). Untreated cells were used as controls. After treatments, medium was removed and Hoechst 33258 was added to each well (10 μg/ml, 15 min). Nuclear morphology and fluorescence were visualized using a Zeiss Axioplan microscope. Digitized images were obtained with a Zeiss Axiocam MRc5 digital camera with the AxiovisionRel 4.4 image software.

Immunofluorescence

Cells were seeded on ibidi (Martinsried, Germany) 4-well μ-slides and treated with 0.5 M sorbitol for 1 h. Untreated cells served as a control group. Then, the cells were fixed with 4% (v/v) formaldehyde in phosphate buffer saline (PBS) pH 7.4 for 15 min at R_T, washed in PBS (x3) and were permeabilized with 0.3 % Triton X-100 for 15 min at R_T. Slides were subsequently blocked with 2% (w/v) BSA for 120 min and incubated overnight with the rabbit polyclonal anti-AQP1 (RA3391/2353) or anti-AQP7 (RA2900/1246) antibodies (1:50 at 4°C). The anti-rabbit IgG-FITC secondary antibody was used at a dilution of 1:100 for 90 min at R_T. Cells were visualized under a Nikon Digital Eclipse C1 confocal laser scanning microscope (Nikon Corporation, Tokyo, Japan).

Light Microscopy

Cells were seeded on ibidi 4-well μ-slides and treated with 0.5 M sorbitol for 1 or 2 h. Untreated cells served as a control group. After washing in PBS (x3) slides were observed with a Zeiss Axio-Observer.Z1 inverted light microscope.

SDS-PAGE and Immunoblot Analysis

Protein samples containing equal amounts of protein (40 μg) were resolved by SDS-PAGE on 8% (w/v) or 10% (w/v) polyacrylamide gels and transferred onto nitrocellulose membranes (0.45 μm). After blocking in TBST (Tris-buffered Saline Tween) containing 5% (w/v) non-fat milk powder (60 min, R_T), the membranes were incubated overnight with the appropriate antibody, according to the manufacturer's instructions (at 1:1000 dilution, except for anti-AQP1 antibody which was used at 1:200 and for anti-AQP7 antibody which was used at 1:500). Following incubation with the respective horseradish peroxidase-conjugated secondary antibody (1:5000 dilution), blots were developed using enhanced chemiluminescence (ECL) and quantified by scanning densitometry (Gel Analyzer v. 1.0). Equal protein loading was verified by re-probing membranes with an anti-actin antibody. Normalization was carried out by dividing the average levels of individual proteins by those of a loading control protein in each sample.

Statistical Analysis

Western blots shown are representative of at least three independent experiments. Data shown correspond to the mean ± SEM and were analyzed by one-way ANOVA multiple comparison test (Graph Pad Prism Software, San Diego, CA) with group comparisons performed using the Bonferroni post-hoc test. $p<0.05$ was considered to indicate a statistically significant difference.

Results

AQP1 and AQP7 mRNA Levels Under Conditions of Hyperosmotic Stress

In accordance with previous studies[1], we first confirmed the expression of AQP1 and AQP7 in H9c2 cardiac myoblasts at the RNA level, by RT-PCR (Figure 1). Sorbitol, at a concentration of 0.5 M, is routinely used as a hyperosmotic stimulus for gene expression studies in cardiomyocyte experimental settings[9]. Interestingly, after treating H9c2 cells with 0.5 M sorbitol for increasing time intervals, ranging from 1 up to 24 hours, we found no apparent change in AQP1 mRNA levels (Figure 1A upper panel). On the other hand, AQP7 mRNA levels were maximally induced at 2 h (5.6 ± 0.47 fold relative to control, $p<0.01$), remaining significantly elevated for at least 6 h (4.79±0.35 fold relative to control, $p<0.01$) (Figure 1A middle panel, B). As a house-keeping gene GAPDH (glyceraldehydes-3-phosphate dehydrogenase) mRNA levels were monitored (Figure 1A bot-

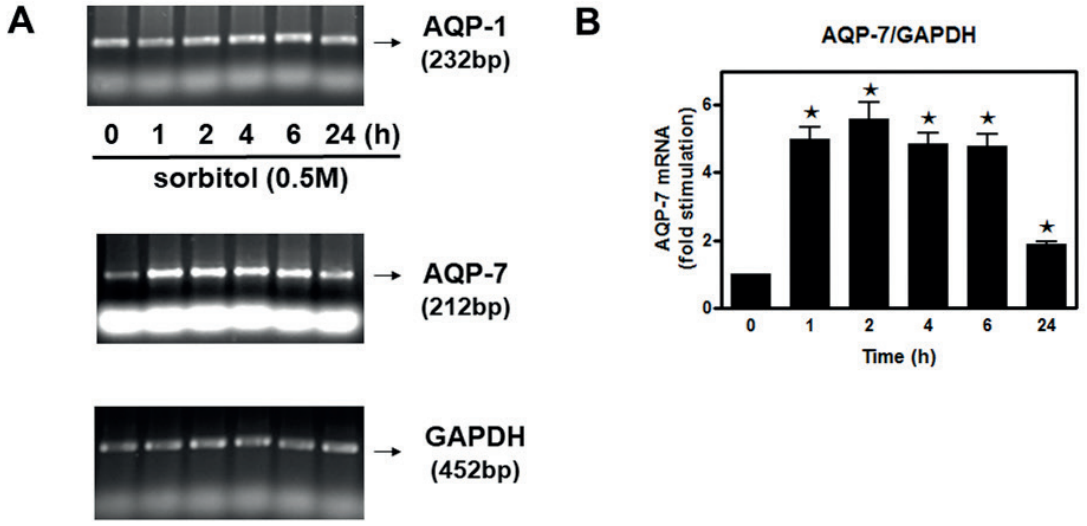

Figure 1. A, Kinetics of hyperosmotic stress-induced AQP1 and AQP7 mRNA upregulation in H9c2 cardiac myoblasts. H9c2 cells were exposed to 0.5 M sorbitol for the times indicated. RNA was extracted and expression of AQP1 (A upper panel), AQP7 (A middle panel) and GAPDH (A bottom panel) mRNA was analyzed by ratiometric RT-PCR. The size of each PCR product is indicated next to the respective panel. After densitometric analysis of the AQP7 PCR product, results were normalized for GAPDH and the data is presented (**B**) as fold stimulation. Results are means ± SEM for at least three independent experiments. * $p<0.01$ compared to control values.

tom panel). Data shown represents densitometric analysis of AQP7 PCR product bands normalized for the respective GAPDH values (Figure 1B).

Protein Expression Pattern of AQP1 and AQP7 Under Conditions of Hyperosmotic Stress

Previous reports[1,6] have demonstrated AQP1 membrane localization in mouse heart and enhanced AQP1 membrane expression under hypotonicity. Therefore, in light of our ratiometric RT-PCR results, we next examined the protein distribution pattern of the AQPs under investigation. Interestingly, immunoreactivity of AQP1 was found to be maximal in the particulate fraction of H9c2 cells treated with sorbitol for 1 hour (2.8±0.30 fold relative to control) (Figure 2A upper panel and B). Antibodies against actin and Gs alpha subunit were used as markers for the cytoplasmic (soluble) and membrane (particulate) fractions, respectively (Figure 2A bottom panels). We did not observe enhanced localization of AQP7 protein to the membrane (Figure 2C).

Immunocytochemical analysis was subsequently performed so as to further investigate and visualize AQP1 and AQP7 protein expression. In accordance with the aforementioned results, the basal immunofluorescent signal corresponding to AQP1 in untreated cells (Figure 3, control), was significantly enhanced after treatment with 0.5 M sorbitol for 1 h (Figure 3, sorbitol 1 h). AQP1 immunoreactivity was detected in the cytoplasm and appeared particularly increased in the peri-nuclear region, possibly indicating its enhanced presence in the endoplasmic reticulum. On the other hand, no significant change was detected in AQP7 immunofluorescent signal, after exposure of H9c2 cells to sorbitol for 1 h (Figure 3).

Hyperosmotic Stress Induces Apoptosis in H9c2 Cells

Studying the morphology of H9c2 cells under conditions of hyperosmotic stress (exposure to 0.5 M sorbitol for 1 and 2 h), we observed their extensive cell shrinkage, due to water efflux (Figure 4).

In line with previous findings reporting induction of apoptosis in cardiac myocytes under these conditions[10], in our hands, exposure of H9c2 cells to 0.5 M sorbitol also triggered apoptosis, as evidenced by cleavage, thus activation, of caspase-3 (Figure 5). In particular, caspase-3 fragmentation was detected from as early as 0.5 h of sorbitol treatment and was maximized after 2 h (3.9±0.3 fold relative to control, $p<0.001$; Figure 5 A upper panel, B). Equal protein loading was verified by re-probing the membrane with an anti-actin antibody (Figure 5A bottom panel).

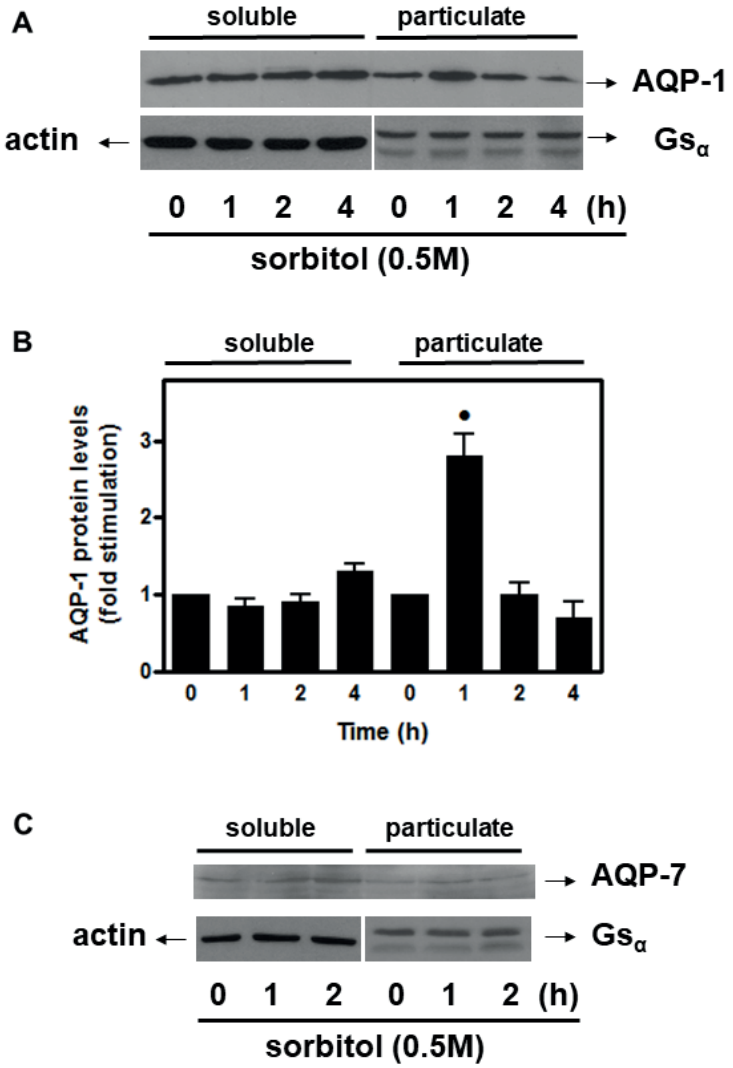

Figure 2. Hyperosmotic stress induces an increase in AQP1 membrane expression but not in that of AQP7. H9c2 cells were exposed to 0.5 M sorbitol for the times indicated. **A,** and **C,** upper panel: Soluble and particulate extracts (40 μg/lane) were subjected to SDS-PAGE and immunoblotted with an antibody for AQP1 (**A**) and AQP7 (**C**). A and C bottom panels: Identical samples were subjected to SDS-PAGE and immunoblotted with an antibody against actin (left) as a marker for soluble extracts and against Gs alpha (right) as a marker for particulate extracts. Western blots presented are representative of at least three independent experiments with overlapping results. Immunoreactive bands were quantified by scanning densitometry and plotted (**B**). Results are means ± SEM for at least three independent experiments. • $p<0.001$ compared to control values.

AQP1 Inhibition Aggravates Apoptosis Triggered by Hyperosmotic Stress in H9c2 Cells

Controversy exists regarding the role of AQP1 in preservation of cell survival, since it can either be beneficial or detrimental, depending on species, cell type and the experimental conditions studied[11-13]. Given the detected enhanced protein expression of AQP1 in sorbitol-treated H9c2 cells, we next sought to determine the anti-survival or pro-survival role of AQP1 in our experimental setting. We thus used $HgCl_2$ which selectively blocks AQP1 activity by binding to Cys^{189} of the protein pore entrance[14]. To avoid any cytotoxic effect, MTT analysis was performed to determine the concentration range of $HgCl_2$ that did not impair H9c2 survival (less than 50 μM, Table I).

Accordingly, H9c2 cells were treated for 30 min with 1 or 25 μM $HgCl_2$, before their exposure to 0.5 M sorbitol. As illustrated in Figure 6 (A upper panel, B), sorbitol-induced PARP proteolysis, an established apoptotic marker[15], was

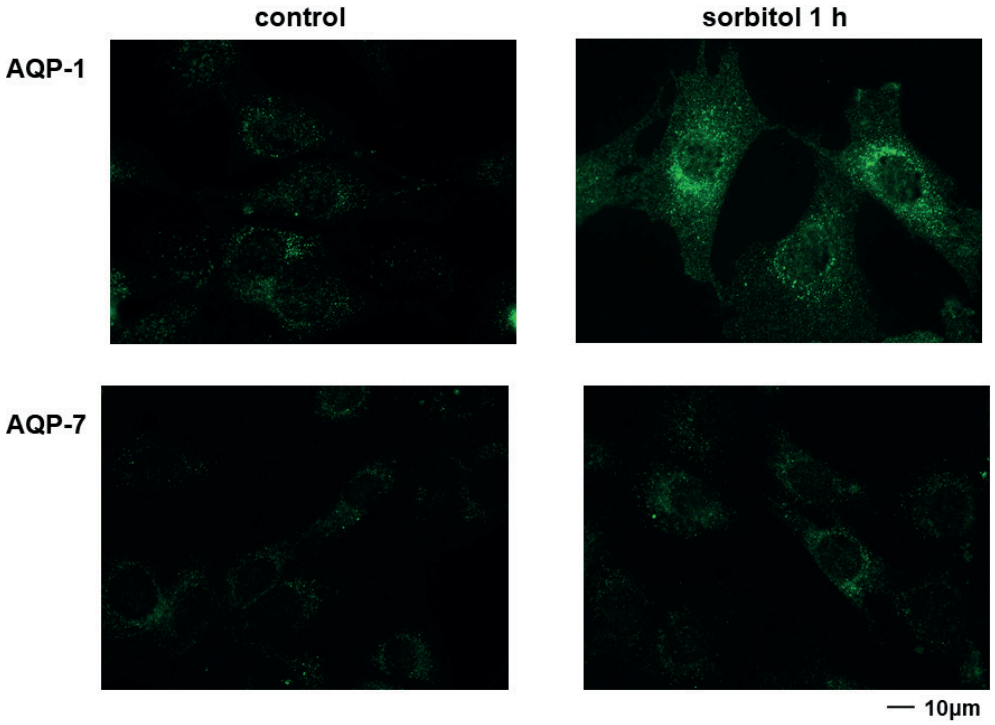

Figure 3. Hyperosmotic stress enhances the membrane localization profile of AQP1 in H9c2 cells. H9c2 cells were left untreated (control) or exposed to 0.5 M sorbitol for 1 h. Cells were then subjected to immunofluorescent analysis with antibodies directed against AQP1 or AQP7 protein levels (green fluorescence). Slides were visualized under a Nikon Digital Eclipse C1 confocal laser scanning microscope. The Figure shows representative photographs for each group, from at least 3 independent experiments. Images were taken at 60x magnification and scale bar: 10 μm.

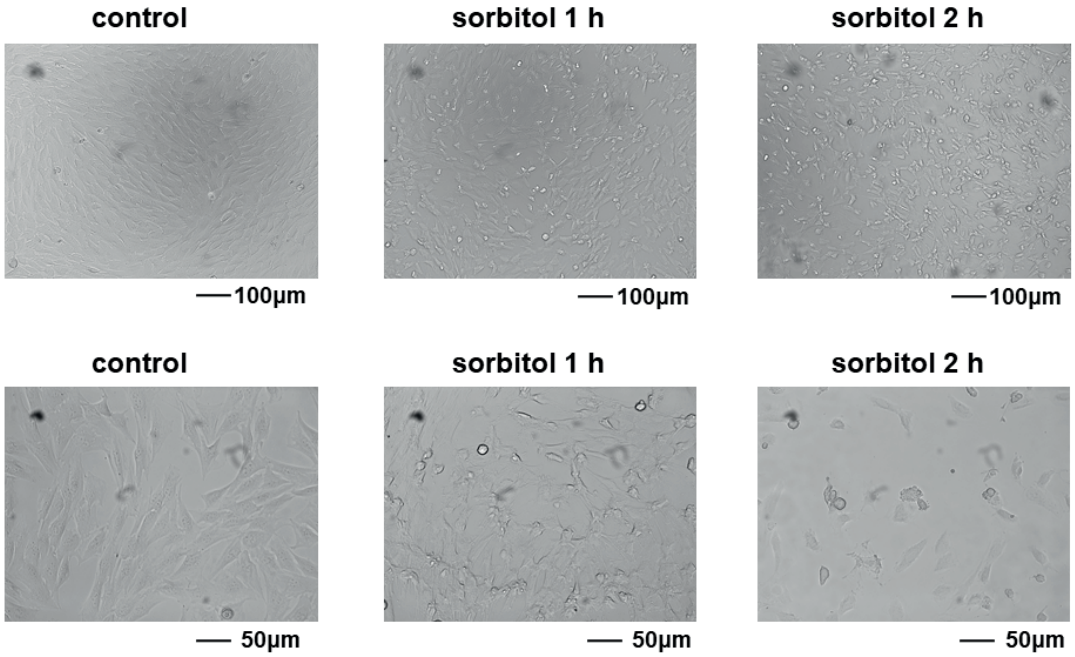

Figure 4. Hyperosmotic stress induces shrinkage and death of H9c2 cells. Cells grown on μ-slides were treated with 0.5 M sorbitol for 1 or 2 h. Untreated cells served as control. Slides were observed with a Zeiss AxioObserver.Z1 inverted light microscope. The Figure shows representative photographs for each group, from at least 3 independent experiments. Images were taken at 10x magnification (scale bar: 100 μm) in upper images or 20X magnification (scale bar: 50 μm) in bottom images.

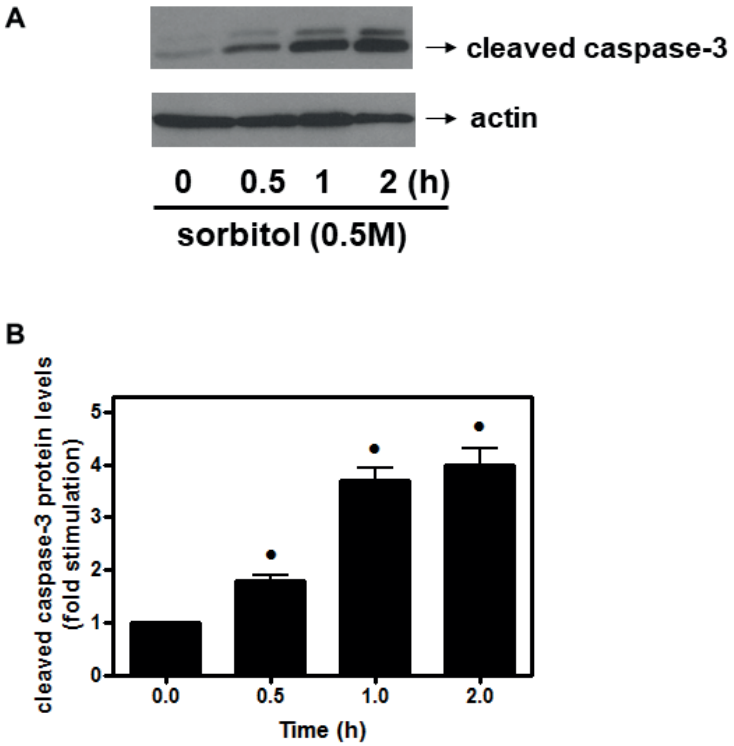

Figure 5. Time-dependent profile of caspase-3 cleavage in response to hyperosmotic stress. **A,** H9c2 cells were exposed to 0.5 M sorbitol for the times indicated. Extracts from cells lysed with Chaps buffer (40 μg) were subjected to SDS-PAGE and immunoblotted with an antibody that recognizes cleaved caspase-3 (A upper panel). Equal protein loading was verified by immunoblotting identical samples with a specific anti-actin antibody (A bottom panel). Western blots are representative of at least three independent experiments with overlapping results. Immunoreactive bands were quantified by scanning densitometry and plotted (**B**). Results are means ± SEM for at least three independent experiments. • $p<0.001$ compared to control values.

enhanced in the presence of 1 μM as well as 25 μM of $HgCl_2$. Equal protein loading was verified by re-probing the membrane with a specific anti-actin antibody (Figure 6A bottom panel). The deleterious effect of AQP1 inhibition was also observed when we probed into caspase-3 fragmentation. In particular, cleaved-caspase-3 protein levels were considerably increased in samples from H9c2 cells treated for 30 min with 25 μM $HgCl_2$, before being exposed to 0.5 M sorbitol (Figure 7 A upper panel, B). Equal protein loading was once again verified by re-probing the membrane with a specific anti-actin antibody (Figure 7A bottom panel). Since apoptosis is also characterized by chromatin condensation[16], we investigated this further by staining H9c2 cells with Hoechst 33258 and observing their nuclear morphology. Indeed, treatment with 0.5 M sorbitol induced a notable upregulation of nuclear fluorescence, compared with the untreated control cells (Figure 8). Chromatin condensation was further enhanced when cells were pre-treated with 25 μM $HgCl_2$ before being exposed to 0.5 M sorbitol (Figure 8).

Discussion

A stable osmotic environment involves normal transport of water and solutes among intracellular and interstitial compartments. Disturbance of osmotic equilibrium results in pathophysiological conditions affecting multiple tissues and organs, including the heart, with myocardial contractility and function being severely compromised[17,18]. Notably, aquaporins are not only important for cardiac water homeostasis, but also for cardiac excitation-contraction coupling, *via* interacting with a number of ion channel proteins and connexins. They have also been tightly associated with infective endocarditis, which can potentially promote human heart valvular destruction, leading to acute heart failure[19]. AQP1 and AQP7 have been

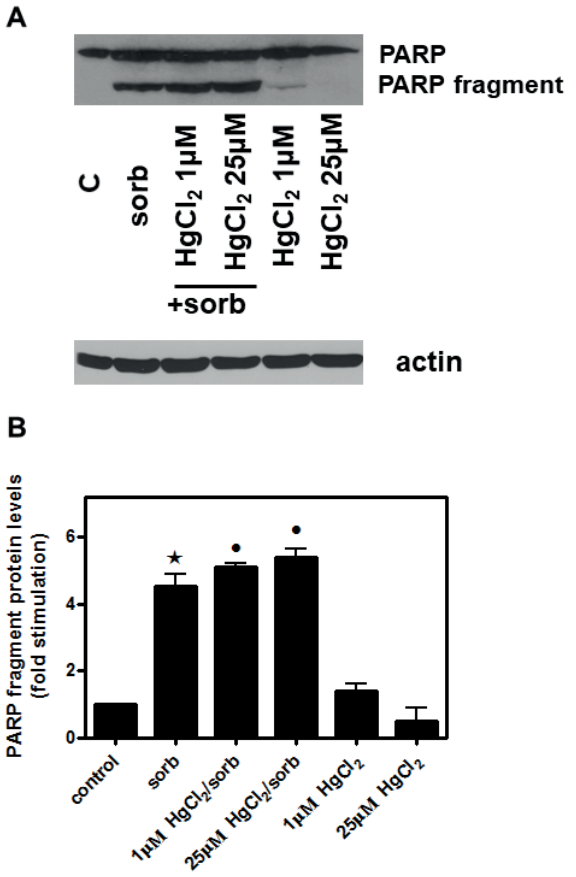

Figure 6. Inhibition of AQP1 activity enhances sorbitol-induced PARP fragmentation in H9c2 cells. **A,** H9c2 cells were left untreated (C: control), or treated with 0.5 M sorbitol (sorb), or incubated with $HgCl_2$ (1 μM or 25μM), or were pre-incubated with $HgCl_2$ (1 μM or 25μM) for 30 min and then exposed to 0.5 M sorbitol (sorb) in the presence of $HgCl_2$. Whole cell extracts (40 μg/lane) were subjected to SDS-PAGE and immunoblotted with an antibody that detects endogenous levels of full length PARP as well as the large 89 kDa PARP fragment (A upper panel). Equal protein loading was verified by immunoblotting identical samples with a specific anti-actin antibody (A bottom panel). Western blots are representative of at least three independent experiments with overlapping results. Immunoreactive bands were quantified by laser scanning densitometry and plotted (**B**). Results are means ± SEM for at least three independent experiments. *p<0.001 compared to control values; •p <0.05 compared to sorbitol-treated cells in the absence of $HgCl_2$.

demonstrated to exert a significant homeostatic role in human cardiovascular physiology. In particular, large scale RNAseq analyses have revealed increased expression of AQP1, AQP7 and AQP3 in samples from healthy donors and patients with dilated cardiomyopathy[20]. In addition, AQP1 has been reported to play a central role in regulation of human heart contractility *via* transport of CO_2[21]. Thus, evaluating the potential of AQPs as stress sensors, prognostic markers or cytoprotective effectors, is of exquisite clinical importance in the context of cardiac cells exposed to the deleterious effects of hyperosmotic stress.

In the present study, in agreement with previous reports[1,5], we detected expression of AQP1 and AQP7 transcripts in H9c2 cardiac myoblasts (Figure 1). Of note, only AQP7 mRNA levels were upregulated significantly after exposure of H9c2 cells to the osmotic insult (Figure 1A middle panel, B). This finding is indicative of a time-dependent regulation of AQP7 mRNA expression under conditions of hyperosmotic stress, not reported before. As far as AQP1 is concerned, in accordance with our results, multiple studies[1,22] have found AQP1 mRNA levels to be constitutive in rat heart. Nevertheless, Rutkovskiy et al[23] have shown that intraperitoneal injection of mice with a hyperosmotic solution, stimulates AQP1 mRNA but not total protein levels in heart. In addition, Jonker et al[24] have demonstrated that both AQP1 mRNA and protein levels are stimulated by hemodilution-induced hypotonic stress in fetal sheep heart.

Subsequently, an effort was made to investigate the protein expression profile of AQP1 and AQP7. We detected enhanced presence of AQP1 in the membrane-associated fraction of H9c2 cells, after treatment with 0.5 M sorbitol (Figure 2A upper panel, B). In addition, our immunocytochemistry experiments demonstrated a significant increase in AQP1 immunofluorescence intensity, in sorbitol-treated H9c2 cells (Figure 3). In agreement with our findings, Umenishi et al[25] showed AQP1 protein expression to be time-dependent, in renal medullar cells exposed to hypertonicity. Furthermore, these results are in accordance with data generated from immunohistochemical studies on primary astrocytes and HEK293 cells treated with hypotonic medium[6].

Noticeably, sorbitol-induced AQP7 mRNA levels were not correlated with an analogously increased protein expression (Figure 2C upper panel). The mechanistic explanation behind this discrepancy remains to be resolved and is a subject of ongoing investigation. Nevertheless, we would like to point out that apoptosis has been previously shown to affect protein synthesis, *via* caspase-mediated cleavage of various factors with translational activity, i.e., polypeptide chain initiation factors (eIF2, eIF4G, eIF4E)[26]. In addition, in a recent study[27], certain short upstream open reading frames (uORFs) were demonstrated to preferentially downregulate translation of spe-

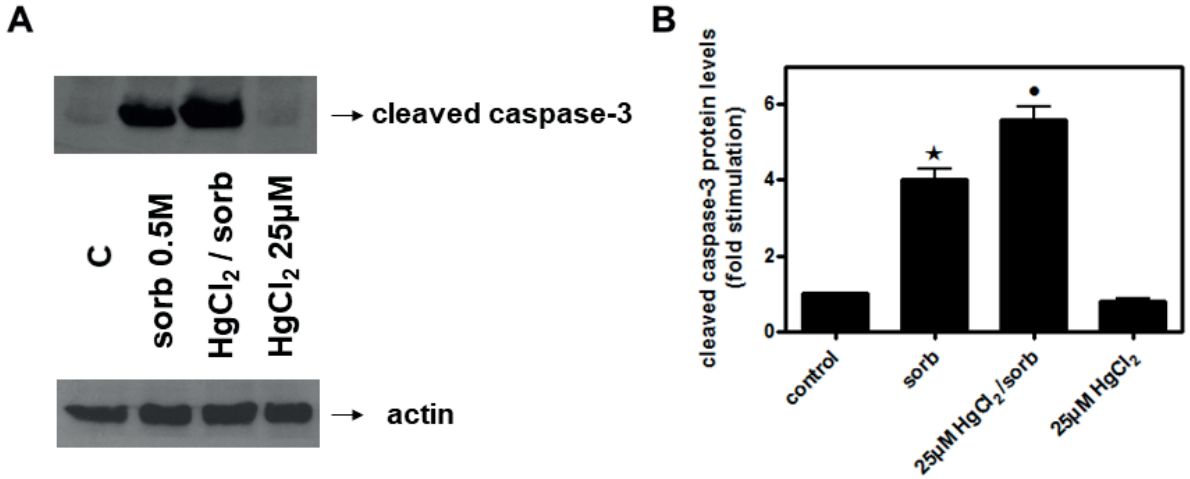

Figure 7. Inhibition of AQP1 activity enhances sorbitol-induced cleavage of caspase-3 in H9c2 cells. **A,** H9c2 cells were left untreated (C: control), or treated with 0.5 M sorbitol (sorb), or incubated with $HgCl_2$ (25μM), or were pre-incubated with $HgCl_2$ (25μM) for 30 min and then exposed to 0.5 M sorbitol (sorb) in the presence of $HgCl_2$. Extracts from cells lysed with Chaps buffer (40 μg) were subjected to SDS-PAGE and immunoblotted with an antibody that recognizes cleaved caspase-3 (A upper panel). Equal protein loading was verified by immunoblotting identical samples with a specific anti-actin antibody (A bottom panel). Western blots are representative of at least three independent experiments with overlapping results. Immunoreactive bands were quantified by scanning densitometry and plotted (**B**). Results are means ± SEM for at least three independent experiments. * $p<0.001$ compared to control values; ● $p<0.05$ compared to sorbitol-treated cells in the absence of $HgCl_2$.

cific mammalian mRNAs, under hyperosmotic stress (i.e., of eIF2D). Failure to correlate mRNA levels with protein expression could thus be attributed to delayed translation of a subset of transcripts, or to the complex and varied post-transcriptional mechanisms that orchestrate mRNA translation[28], particularly under stress. Overall, in our experimental setting, the expression of aquaporin family members is upregulated by hyperosmotic stress, either at the transcriptional (AQP7), or at the translational (AQP1) level.

After verifying that the hyperosmotic insult triggers apoptosis in our experimental setting (Figure 5), we looked into the role of the highly expressed AQP1 under these conditions, using $HgCl_2$. Mercuric chloride, in concentrations varying from 5 up to 300 μM[30], constitutes a general inhibitor of most AQPs[29]. AQP1 and AQP2 are specifically sensitive to $HgCl_2$, in contrast to AQP7 and AQP4, which are insensitive to this compound[14]. With AQP2 being the principal aquaporin in kidney and AQP1 and AQP7 being expressed and active in cardiac muscle[5], any effect seen in H9c2 cells in the presence of $HgCl_2$, can be attributed to blockade of AQP1 activity. Thus, the enhancement of sorbitol-induced apoptosis in the presence of $HgCl_2$, as evidenced by a considerable increase in PARP (Figure 6) and caspase-3 fragmentation (Figure 7), as well as in chromatin condensation (Figure 8), is indicative of a salutary role of AQP1, in our experimental setting. This finding is of fundamental significance, since it underlies the cytoprotective function of AQP1, as a sensor of- and responder to hyperosmotic stress in H9c2 cells. In agreement with our observation, AQP1 has been found to exert a cytoprotective effect by alleviating myocardial edema after cardiopulmonary bypass in sheep[31] and by reversing LPS-induced apoptosis in HK-2 renal epithelial cells[32]. In addition, AQP1 overexpression suppresses hyperglycemia-induced apoptosis in endothelial cells[33]. Inhibition of AQP1 expression also augments apoptosis of human lens epithelial cells, promoting development of cataracts[13]. On the other hand, Li et al[3] have found AQP1 deficiency to protect against myocardial infarction in mice. AQP1 ablation also exerts a pro-survival effect in ischemic goat heart[34], as well as in rat heart after cardiopulmonary bypass[35].

Collectively, our study unveils the response mechanisms of AQP1 and AQP7 in H9c2 cells exposed to hyperosmotic stress, as well as the salutary effect of AQP1 against the apoptotic death triggered (Figure 9). Promoting cardiac cells survival is nodal in preservation of cardiac homeostatic equilibrium. Therefore, future researches are required in order

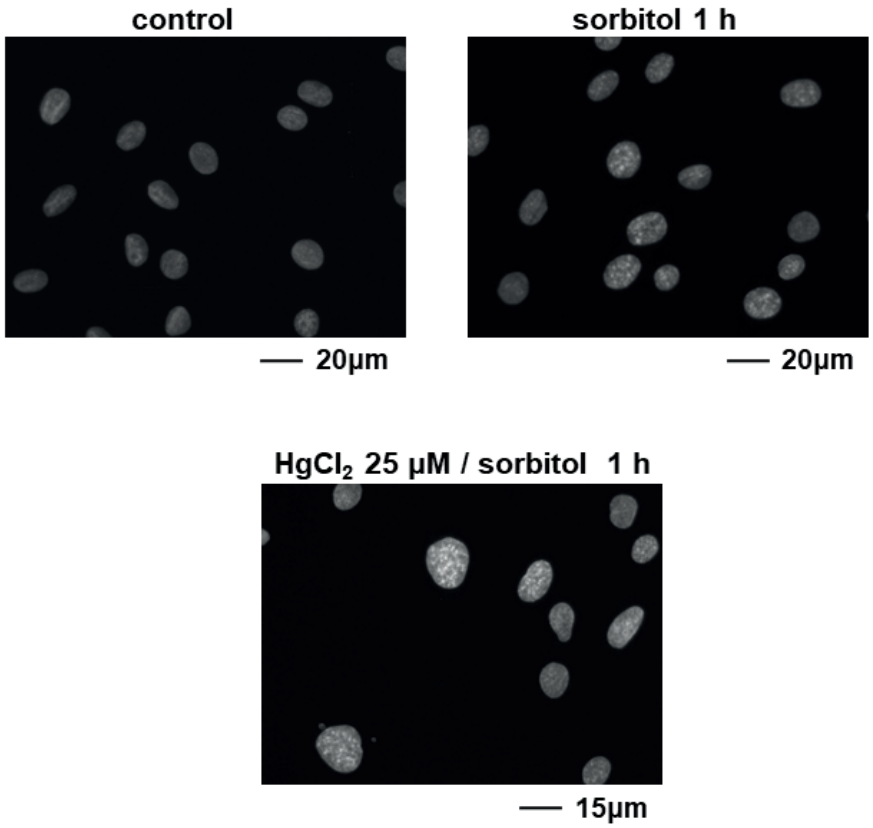

Figure 8. Hyperosmotic stress stimulates chromatin condensation in H9c2 cells. Chromatin condensation, indicative of apoptosis, was detected using the Hoechst staining method. Cells were cultured onto µ-slides and treated with 0.5 M sorbitol for 1 h in the presence or absence of 25 µM $HgCl_2$. Untreated cells served as a control group. Hoechst 33258 (10 µg/ml) was added and after cells were washed three times with PBS, nuclear morphology and fluorescence were visualized using a Zeiss Axioplan microscope. The Figure shows representative photographs for each group from at least 3 independent experiments. Scale bar: 20 or 15 µm, as indicated.

to further clarify and define the physiological roles that aquaporins play in the context of the human myocardium. In light of the numerous pathophysiological conditions involving osmotic imbalances (ischemia/reperfusion, diabetes, myocardial edema, septic shock etc.), designing and promoting novel therapeutic strategies is of outmost importance, so as to limit patients' morbidity and mortality. Given the complexity of the molecular mechanisms mediating aquaporins expression, localization and function, data from different experimental settings (cell lines, primary cells and *ex vivo* models) are needed before extrapolating any scientific outcome to the milieu of the human myocardium.

Conclusions

In the present study, AQPs were found to be differentially regulated under hyperosmotic stress conditions induced by sorbitol, in H9c2 cardiac myoblasts. The core findings of this study are as follows:

- Hyperosmotic stress upregulates AQP7 expression at the transcriptional level, in a time-dependent manner.
- Hyperosmotic stress enhances AQP1 membrane-associated protein levels, in a time-dependent manner.
- AQP1 functions as a response factor and sensor of osmotic stress in H9c2 cells.
- AQP1 exerts a salutary role against apoptosis conferred by hyperosmotic stress in H9c2 cells.

Author Contributions
Conceptualization, I.-K.A.; Data curation, I.-K.A., A.K. and F.P.; Formal analysis, I.-K.A.; Funding acquisition, I.-K.A., C.G.; Project administration, I.-K.A.; Supervision, I.-K.A.; Validation, I.-K.A.; Writing – original draft, I.-K.A.; Writing – review & editing, C.G.

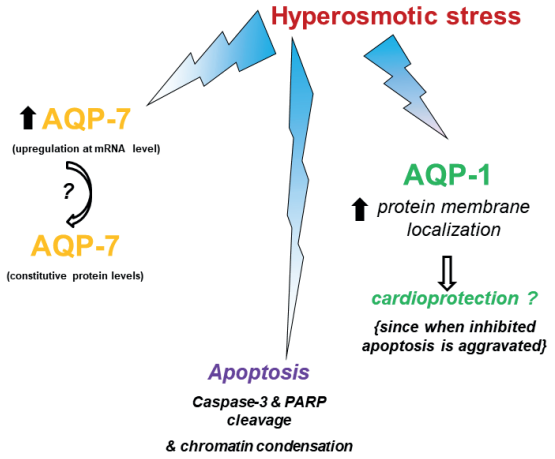

Figure 9. Schematic diagram of a model depicting the responses of AQP1 and AQP7 in H9c2 cells exposed to hyperosmotic stress.

Funding

This work was funded by a Special Research Account of the National and Kapodistrian University of Athens grant (K.A. 70/4/11242).

Acknowledgments

We thank Prof. S. Nielsen (University of Aarhus, Aarhus, Denmark) for kindly providing us with the anti-AQP1 (RA3391/2353) and anti-AQP7 antibodies (RA2900/1246). The authors are also grateful to Ass. Prof. M.H. Antonelou for advice and donation of reagents, as well as to Dr A.D. Velentzas for his help with the confocal microscope. This study was funded by a Special Research Account of the National and Kapodistrian University of Athens grant (K.A. 70/4/11242).

Conflict of Interest

The Authors declare that they have no conflict of interests.

References

1) Butler TL, Au CG, Yang B, Egan JR, Tan YM, Hardeman EC, North KN, Verkman AS, Winlaw DS. Cardiac aquaporin expression in humans, rats, and mice. Am J Physiol Heart Circ Physiol 2006; 291: H705-H713.
2) Egan JR, Butler TL, Au CG, Tan YM, North KN, Winlaw DS. Myocardial water handling and the role of aquaporins. Biochim Biophys Acta 2006; 1758: 1043-1052.
3) Li L, Weng Z, Yao C, Song Y, Ma T. Aquaporin-1 deficiency protects against myocardial infarction by reducing both edema and apoptosis in mice. Sci Rep 2015; 5: 13807-13816.
4) Alleva K, Chara O, Amodeo G. Aquaporins: another piece in the osmotic puzzle. FEBS Lett 2012; 586: 2991-2999.
5) Rutkovskiy A, Valen G, Vaage J. Cardiac aquaporins. Basic Res Cardiol 2013; 108: 393-411.
6) Conner MT, Conner AC, Bland CE, Taylor LH, Brown JE, Parri HR, Bill RM. Rapid aquaporin translocation regulates cellular water flow: mechanism of hypotonicity-induced subcellular localization of aquaporin 1 water channel. J Biol Chem 2012; 287: 11516-11525.
7) Hibuse T, Maeda N, Nakatsuji H, Tochino Y, Fujita K, Kihara S, Funahashi T, Shimomura I. The heart requires glycerol as an energy substrate through aquaporin 7, a glycerol facilitator. Cardiovasc Res 2009; 83: 34-41.
8) Hoffmann EK, Lambert IH, Pedersen SF. Physiology of cell volume regulation in vertebrates. Physiol Rev 2009; 89: 193-277.
9) Clerk A, Kemp TJ, Harrison JG, Mullen AJ, Barton PJR, Sugden PH. Up-regulation of c-jun mRNA in cardiac myocytes requires the extracellular signal-regulated kinase cascade, but c-Jun N-terminal kinases are required for efficient up-regulation of c-Jun protein. Biochem J 2002; 368: 101-110.
10) Eisner V, Quiroga C, Criollo A, Eltit JM, Chiong M, Parra V, Hidalgo K, Toro B, Díaz-Araya G, Lavandero S. Hyperosmotic stress activates p65/RelB NFkappaB in cultured cardiomyocytes with dichotomic actions on caspase activation and cell death. FEBS Lett 2006; 580: 3469-3476.
11) Song D, Yang Y, He N, Tian X, Sang DS, Li YJ. The involvement of AQP1 in myocardial edema induced by pressure overload in mice. Eur Rev Med Pharmacol Sci 2018; 22: 4969-4974.
12) Venglovecz V, Pallagi P, Kemény LV, Balázs A, Balla Z, Becskeházi E, Gál E, Tóth E, Zvara Á, Puskás LG, Borka K, Sendler M, Lerch MM, Mayerle J, Kühn J-P, Rakonczay Z Jr, Hegyi P. The importance of aquaporin 1 in pancreatitis and its relation to the CFTR Cl- channel. Front Physiol 2018; 9: 1-15.
13) Zheng HH, Xu GX, Guo J, Fu LC, Yao Y. Aquaporin-1 down regulation associated with inhibiting cell viability and inducing apoptosis of human lens epithelial cells. Int J Ophthalmol 2016; 9: 15-20.
14) Preston GM, Jung JS, Guggino WB, Agre P. The mercury-sensitive residue at cysteine 189 in the CHIP28 water channel. J Biol Chem 1993; 268: 17-20.
15) Soldani C, Scovassi AI. Poly(ADP-ribose) polymerase-1 cleavage during apoptosis: an update. Apoptosis 2002; 7: 321-328.
16) Konstantinidis K, Whelan RS, Kitsis RN. Mechanisms of cell death in heart disease. Arterioscler Thromb Vasc Biol 2012; 32: 1552-1562.
17) Galvez A, Morales MP, Eltit JM, Ocaranza P, Carrasco L, Campos X, Sapag-Hagar M, Díaz-Araya G, Lavandero S. A rapid and strong apoptotic process is triggered by hyperosmotic stress in cultured rat cardiac myocytes. Cell Tissue Res 2001; 304: 279-285.

18) Wright AR, Rees SA. Cardiac cell volume: crystal clear or murky waters? A comparison with other cell types. Pharmacol Ther 1998; 80: 89-121.
19) Benoit M, Thuny F, Le Priol Y, Lepidi H, Bastonero S, Casalta J-P, Collart F, Capo C, Raoult D, Mege J-L. The transcriptional programme of human heart valves reveals the natural history of infective endocarditis. PLoS One 2010; 5: e8939.
20) Heinig M, Adriaens ME, Schafer S, Van Deutekom HWM, Lodder EM, Ware JS, Schneider V, Felkin LE, Creemers EE, Meder B, Katus HA, Rühle F, Stoll M, Cambien F, Villard E, Charron P, Varro A, Bishopric NH, George Jr. AL, dos Remedios C, Moreno-Moral A, Pesce F, Bauerfeind A, Rüschendorf F, Rintisch C, Petretto E, Barton PJ, Cook SA, Pinto YM, Bezzina CR, HubnerN. Natural genetic variation of the cardiac transcriptome in non-diseased donors and patients with dilated cardiomyopathy. Genome Biol 2017; 18: 170.1-170.8.
21) Miller RT. Aquaporin in the heart – only for water? J Mol Cell Cardiol 2004; 36: 653-654.
22) Tabbut S, Nelson DP, Tsai N, Miura T, Hickey PR, Mayer JE, Neufeld EJ. Induction of aquaporin-1 mRNA following cardiopulmonary bypass and reperfusion. Mol Med 1997; 3: 600-609.
23) Rutkovskiy A, Mariero LH, Nygård S, Stensløkken KO, Valen G, Vaage J. Transient hyperosmolality modulates expression of cardiac aquaporins. Biochem Biophys Res Commun 2012; 425: 70-75.
24) Jonker SS, Davis LE, van derBilt JDW, Hadder B, Hohimer AR, Giraud GD, Thornburg KL. Anaemia stimulates aquaporin 1 expression in the feat; sheep heart. Exp Physiol 2003; 88: 691-698.
25) Umenishi F, Schrier RW. Hypertonicity-induced aquaporin-1 (AQP1) expression is mediated by the activation of MAPK pathways and hypertonicity-responsive element in the AQP1 gene. J Biol Chem 2003; 278: 15765-15770.
26) Morley SJ, Coldwell MJ, Clemens MJ. Initiation factor modifications in the preapoptotic phase. Cell Death Differ 2005; 12: 571-584.
27) Akulich KA, Sinitcyn PG , Makeeva DS, Andreev DE , Terenin IM , Anisimova AS , Shatsky IN, Dmitriev SE . A novel uORF-based regulatory mechanism controls translation of the human MDM2 and eIF2D mRNAs during stress. Biochimie 2019; 157: 92-101.
28) Greenbaum D, Colangelo C, Williams K, Gerstein M. Comparing protein abundance and mRNA expression levels on a genomic scale. Genome Biology 2003; 4: 117.1-117.8
29) Beitz E, Golldack A, Rothert M, von Bülow J. Challenges and achievements in the therapeutic modulation of aquaporin functionality. Pharmacol Ther 2015; 155: 22-35.
30) Jablonski EM, Webb AN, McConnell NA, Riley MC, Hughes FMJr. Plasma membrane aquaporin activity can affect the rate of apoptosis but is inhibited after apoptotic volume decrease. Am J Physiol Cell Physiol 2004; 286: C975-C985.
31) Ding FB, Yan YM, Bao CR, Huang JB, Mei J, Liu H, Ma N, Zhang JW. The role of aquaporin 1 activated by cGMP in myocardial edema caused by cardiopulmonary bypass in sheep. Cell Physiol Biochem 2013; 32: 1320-1330.
32) Wang Y, Zhang W, Yu G, Liu Q, Jin Y. Cytoprotective effect of aquaporin 1 against lipopolysaccharide-induced apoptosis and inflammation of renal epithelial HK-2 cells. Exp Ther Med 2018; 15: 4243-4252.
33) Sada K, Nishikawa T, Kukidome D, Yoshinaga T, Kajihara N, Sonoda K, Senokuchi T, Motoshima H, Matsumura T, Araki E. Hyperglycemia induces cellular hypoxia through production of mitochondrial ROS followed by suppression of aquaporin-1. PLOS one 2016; 11: e0158619.
34) Ding FB, Yan YM, Huang JB, Mei J, Zhu JQ, Liu H. The involvement of AQP1 in heart oedema induced by global myocardial ischemia. Cell Biochem Funct 2013; 31: 60-64.
35) Song D, Liu X, Diao Y, Sun Y, Gao G, Zhang T, Chen K, Pei L. Hydrogen-rich solution against myocardial injury and aquaporin expression via the PI3K/Akt signaling pathway during cardiopulmonary bypass in rats. Mol Med Rep 2018; 18: 1925-1938.